Air-Stable n-Doped Colloidal HgS Quantum Dots

ARTICLE *in* JOURNAL OF PHYSICAL CHEMISTRY LETTERS · MARCH 2014

Impact Factor: 7.46 · DOI: 10.1021/jz500436x

THE JOURNAL OF PHYSICAL CHEMISTRY Letters

Letter

pubs.acs.org/JPCL

Air-Stable n-Doped Colloidal HgS Quantum Dots

Kwang Seob Jeong, Zhiyou Deng, Sean Keuleyan, Heng Liu, and Philippe Guyot-Sionnest*

The James Franck Institute, 929 East 57th Street, The University of Chicago, Chicago, Illinois 60637, United States

Supporting Information

ABSTRACT: HgS nanocrystals show a strong mid-infrared absorption and a bleach of the near-infrared band edge, both tunable in energy and reversibly controlled by exposure to solution ions under ambient conditions. The same effects are obtained by applying a reducing electrochemical potential, confirming that the mid-infrared absorption is the intraband transition of the quantum dot. This is the first time that stable carriers are present in the quantum state of strongly confined quantum dot in ambient conditions. The mechanism by which doping is achieved is attributed to the rigid shifts of the valence and conduction band with respect to the environment, similar to the sensitivity of the work function of surfaces to adsorbates.

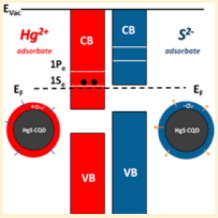

SECTION: Physical Processes in Nanomaterials and Nanostructures

There is much interest in controlling the doping of colloidal quantum dots for applications such as light emitting devices, solar cells, photodetectors or electronics.[1] Impurity doping[2,3] as in bulk, or charge transfer doping[4] are the main approaches. Most applications do not need the Fermi level to be moved into the quantum dot interior states, and tuning it up or down within the gap is sufficient to create pn junctions, albeit the optimum junction may require the largest excursion of the Fermi level. There is also interest in using colloidal quantum dot for infrared applications. Competing with small gap infrared materials, there should be a possibility of using the intraband transitions of established wide gap semiconductors. To use intraband transitions, it then becomes imperative to have carriers occupy the quantum dot states, which is again a doping problem. However, for any quantum dot in the strongly confined regime, moving the Fermi level so extensively has not yet been achieved by impurity doping, as evidenced by the lack of the intraband transitions, while it has been achieved by charge transfer only in inert conditions. This report on β-HgS shows a first case of strongly confined quantum dots where carriers are stably in the lowest conduction band state under ambient conditions. The doping is controlled by the surface and explained by a rigid shift of the quantum states with respect to the environment.

HgS nanocrystals were synthesized in organic solvent following a variant of the synthesis developed for HgTe nanocrystals[5] described in Supporting Information (SI). The HgS nanocrystals initially prepared in oleylamine are then capped with dodecanethiols. After precipitation, they are dissolved in tetrachloroethylene or toluene. They are roughly spherical as shown in Figure 1A. HgS exists in two forms at room temperature; the black zinc blende β-HgS, metacinnabar, and the red hexagonal α-HgS, cinnabar. Cinnabar is the stable bulk form at room temperature but chemical precipitation methods yield β-HgS as shown in Figure 1B. Figure 1C shows absorption spectra for HgS nanocrystals of ~5 nm diameter in a tetrachloroethylene solution, in ambient conditions. There is a strong mid-IR absorption, around 2000 cm^{-1}, which is very well isolated from the near-IR (NIR) edge at ~9000 cm^{-1}, and it was first noticed that the spectra were sensitive to the ligands. Subsequently, applying a layer by layer growth[6] with Hg^{2+} ($HgCl_2$ or $Hg(CH_3CO_2^-)_2$ provide the same results) and S^{2-}, using $(NH_4)_2S$, the particles are grown larger, monolayer by monolayer, but the spectra change completely. The sulfide redshifts the NIR edge and removes the mid-IR absorption, while the Hg^{2+} blue shifts the NIR edge and induces the mid-IR absorption. The transfer of oscillator strength between the NIR edge and the mid-IR absorption is quantitative, systematic and irrespective of the order of surface exposure to the ions. Inductively coupled plasma optical emission spectrometry confirms changes in composition of the Hg treated and S treated HgS CQDs (Table 1-SI) while the spectral features globally redshift consistent with particle growth. Such spectral effects have been seen before for quantum dots CdSe, ZnO, PbSe, HgTe,[4,7,8] but only with charge transfer. It is therefore proposed that the β-HgS quantum dots can be stably doped, but for the first time, controlled by the surface and in ambient conditions such that they exhibit a stable intraband absorption. Since HgS has not been much studied as a colloidal quantum dot, we used spectroelectrochemistry to (i) determine the sign of the carrier, (ii) verify the quantum confinement of the nanocrystals, (iii) determine the bandgap, and (iv) understand the mechanism of doping.

For spectroelectrochemistry, HgS nanocrystals of different average sizes from ~3.5 to ~14 nm were deposited as a film on a Pt electrode. They were cross-linked by hexanedithiol to render them insoluble in the electrolyte and improve electron transfer.[9] Figure 2A shows difference infrared spectra between various potentials and +1.2 V with respect to the pseudo reference electrode Ag/AgCl for the smallest sample of average size ~3.5 nm. As the potential is moved to the negative direction, the mid-IR absorption starts around 2350 cm^{-1}, and

Received: March 1, 2014
Accepted: March 17, 2014
Published: March 17, 2014

   dx.doi.org/10.1021/jz500436x | J. Phys. Chem. Lett. 2014, 5, 1139−1143

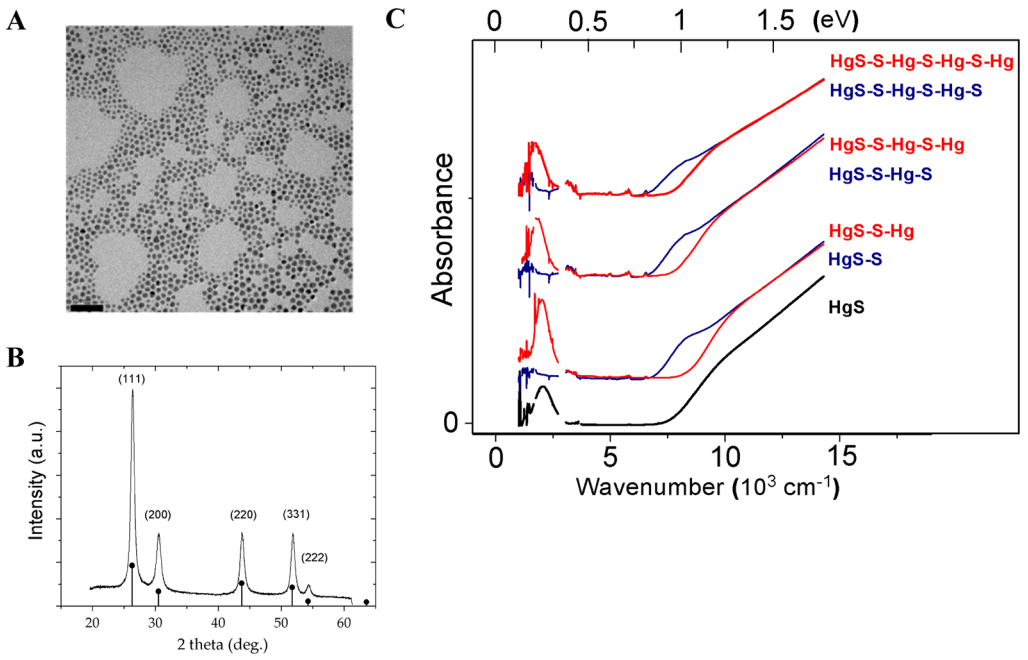

Figure 1. (A) TEM image of HgS CQDs. The average size is 6.4 nm and the standard deviation is 1.3 nm. Scale bar is 50 nm. (B) X-ray diffraction spectrum. Bulk β-HgS peak positions are indicated. (C) Spectra of ~5 nm HgS dots with alternating S^{2-} and Hg^{2+} layer by layer growth. The HgS (black) corresponds to the untreated dots, and S (blue) and Hg (red) represents the S^{2-} and Hg^{2+} surface treatments, respectively. Vibrational absorptions were omitted for clarity. The full spectra are in Figure S1 (Supporting Information).

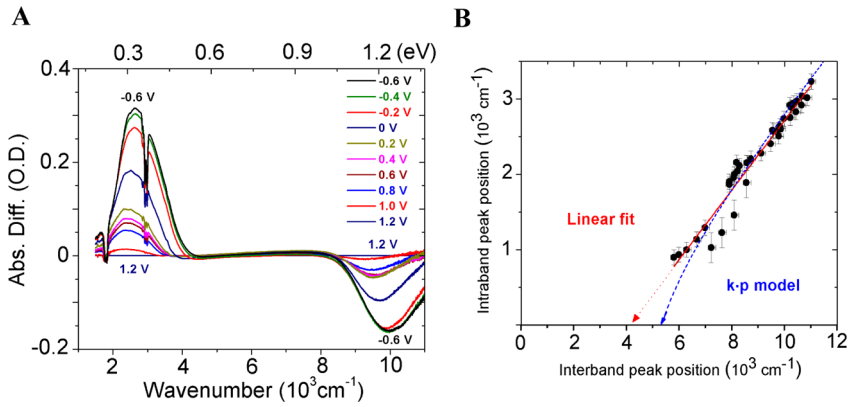

Figure 2. (A) Difference spectra of a film HgS CQD under increasingly negative potential vs Ag/AgCl. The spectrum at +1.2 V is used as the reference. (B) Mid-IR peak (Intraband) vs NIR peak (Interband) energies. The red line is a linear fit and the blue line is the $k{\cdot}p$ prediction.

gains strength as it moves toward 2600 cm^{-1} at the most negative potential, −0.6 V. At the same time, the NIR shows a bleach that increases for the more negative potentials. The transfer of oscillator strength is similar to the observations described above for the layer by layer modification in solution and typical of previous spectroelectrochemical studies on strongly confined quantum dots. The fact that the intraband transition appears for negative potential allows its assignment to the conduction band and the doping as n-type.

To determine the extent to which the carriers are quantum confined, we investigated the tuning of the energy of the spectral features. By taking difference spectra every 100 mV, the mid-IR absorption and NIR bleach show well-defined Gaussian peaks. Figure 2B shows the complete set of the peaks of mid-IR absorption as a function the peaks of the NIR bleach. The NIR bleach blueshifts with smaller sizes, covering a range of more than 0.6 eV. This is the evidence that the HgS nanocrystals are strongly quantum confined.

A linear extrapolation of the intraband energy to zero would give a bandgap of 0.51 ± 0.04 eV. A linear extrapolation would be justified only in the effective mass approximation but assigning the intraband absorption to the $1S_e-1P_e$ electronic transition for a spherical dot gives a slope of ~1, which fails to describe the data. The nonparabolic approximation, specifically a two band $k{\cdot}p$ model, (described in the SI) captures the data better with no other parameter than the bandgap value of 0.66 eV. We note that the bulk bandgap of β-HgS is very uncertain in the literature with experimental values between −0.5 eV and +0.5 eV.[10] Weller and co-workers synthesized β-HgS in aqueous solutions, with absorption and luminescence in the near-infrared[11] and stated a bulk bandgap of +0.5 eV[12] while Kuno and co-workers synthesized smaller particles in organic solvents with fluorescence in the visible[13] and stated the band gap as negative, but neither reports measured the bulk gap. There is theoretical interest in β-HgS as well, as a topological insulator,[14] but the calculated bulk gaps also range from

dx.doi.org/10.1021/jz500436x | J. Phys. Chem. Lett. 2014, 5, 1139−1143

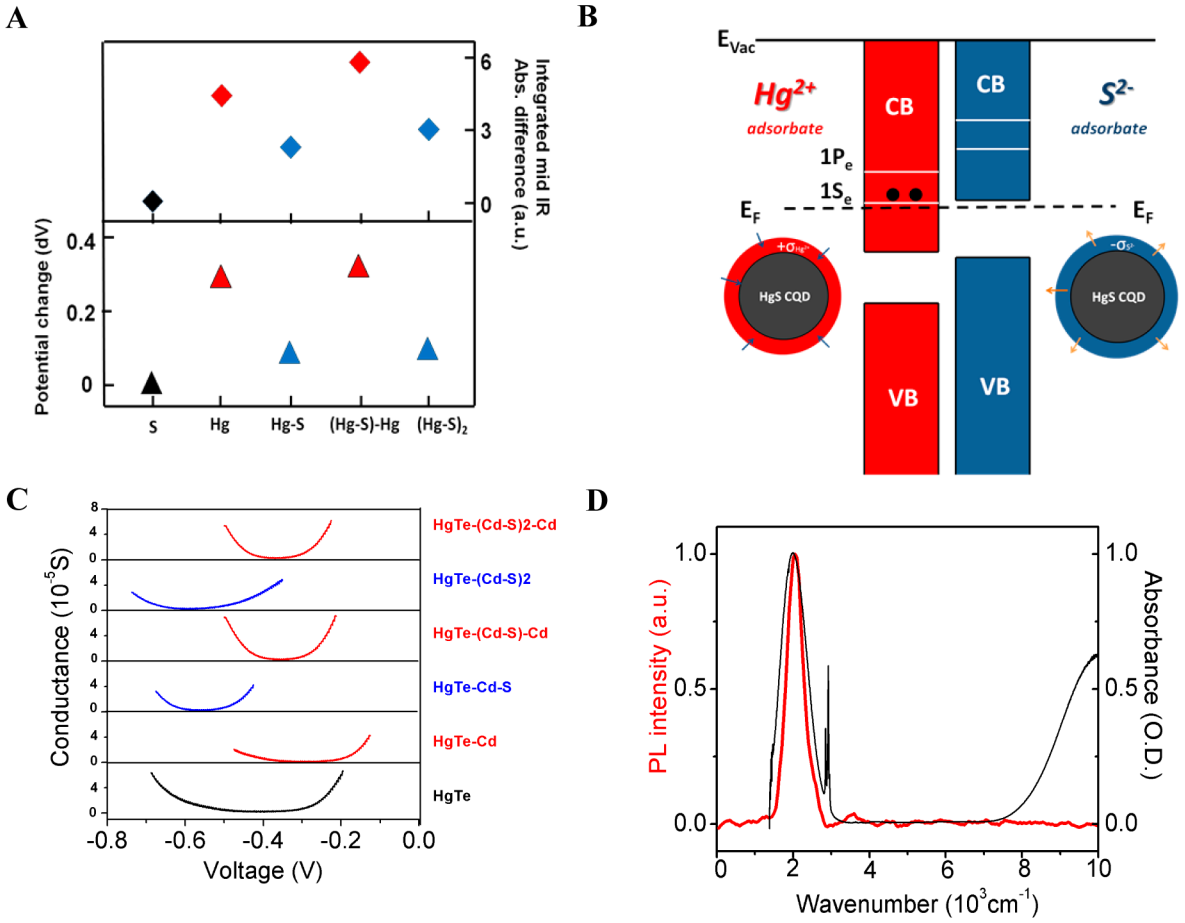

Figure 3. (A) Resting potential difference and integrated mid-infrared absorption of a HgS CQD film after alternate exposure to Hg^{2+} and S^{2-} ions, relative to the first measurement of the ethanedithiol cross-linked HgS CQD film. The resting potential is measured 40 s after immersion in the electrolyte. (B) Schematic energy diagrams of the Hg^{2+}-doped and the S^{2-}-treated HgS CQDs. (C) Shift of the conductance curve for HgTe CQD films with alternating exposure to Cd^{2+} and S^{2-}. (D) Intraband photoluminescence emission (red) from the $1S_e-1P_e$ transition of ambient n-type HgS nanocrystals after photoexcitation at 808 nm. The absorption spectrum (black) is overlapped with the photoluminescence emission spectrum (red).

negative to positive values. The band gap of ~0.6 eV measured here is similar to the value stated by Weller and co-workers.[12]

Using interdigitated electrodes, the electrochemistry also confirms that the injected electrons are conductive as expected from many prior studies on other quantum dot solids, while cyclic voltammetry (Figure S1) shows the typical waveform expected for nearly reversible charge injection. It is noted that no electrochromic effects and no conductivity are obtained in the oxidizing direction, indicating that p-type HgS CQDs are not stable, most likely because holes oxidize the surface. Thus, unlike HgTe, HgS is not ambipolar.

The mechanism of how n-type dots are air-stable and created by the surface exposure to Hg^{2+} is now discussed. The n-type doping of HgS CQD cannot be explained by charge transfer from the adsorbate, or by the electronegativity of the adsorbate since the electronegative sulfide (S^{2-}) instead removes the electrons from the dots as shown in Figure 1C. An alternative possibility is that the surface introduces an energy shift of the nanocrystal states with respect to the environment, stabilizing the doping. The surface can indeed affect the reduction potential of quantum dots by changing the electrostatic potential. For example, changes in transport of CdSe nanowire FETs after exposure to solutions of sulfide or metal ions and subsequent thermal processing have been reported and it has been proposed that the surface composition plays an important role in doping.[15] The use of surface ligands to optimize the $p-n$ junction in nanocrystal films has been reported as well.[16]

To investigate whether the potential of the dots varied with surface modifications, the resting potential of a ethanedithiol cross-linked HgS CQD film on a Pt wire was measured with respect to an Ag/AgCl pseudoreference in a formamide/tetrabulyammonium perchlorate electrolyte. The wire was alternately exposed to mercury or sulfide ions solutions, rinsed and dried. The data in Figure 3A show alternating resting potentials between ca. 0 and ca. +300 mV with the positive potentials after mercury ions exposure. On films deposited on an IR transparent CaF_2 substrate but processed in the same manner, the strength of the intraband absorption of the film also alternates with the mercury and sulfide treatment. Unlike for the solutions in Figure 1C, the intraband absorption in the film is not as completely quenched by sulfur (Figure S5), which is tentatively attributed to the different environment (polar electrolyte vs nonpolar solvent) and accessibility in the film but the trends are similar.

Figure 3A shows the strong correlation of both measurements as a function of the surface exposure. Therefore, these measurements confirm the idea that the surface moves the energy levels with respect to the environment rather than serves

dx.doi.org/10.1021/jz500436x | J. Phys. Chem. Lett. 2014, 5, 1139−1143

as a dopant. Effectively, the surface tunes the redox potential of the nanocrystals.[17] Campbell et al. showed how a work function can shift by 1 V in air with dipolar self-assembled monolayers.[18] As shown in Figure 3B, a surface dipole pointing inward (positive end on the surface) raises the electric potential inside (+ V) which stabilizes the electron (− eV) and increases the work function. For a sphere with a radius much larger than the dipole layer thickness, the energy shift is $\Delta E_f = \sigma_d / \varepsilon\varepsilon_0$ (eV) where σ_d is the surface dipole density with the positive direction toward outside and ε is the dielectric constant in the dipole layer. The effect can be large. Assuming that the surface dipole due to the ions alternates between +1 D and −1 D pointing outside the particle, and that each ion occupies a surface of 20 Å^2, as an estimated surface coverage of ions on the (111) plane, using the smallest screening with $\varepsilon = 1$, the energy shift is $\sim \pm$ 1.8 eV.

The alternating Hg^{2+} and S^{2-} additions lead to surface dipole layers of varying magnitude or polarity. A dipole pointing from the ligands to Hg^{2+} lowers the quantum dot states with respect to the outside, while the dipole from S^{2-} to the ligands raises them (Figure 3B). The occupation of the electronic states is determined by the Fermi level of the environment and shifting the dot electron state quantum state above (S^{2-}) and below (Hg^{2+}) leads to the doping observed. The electrostatic shift captures the essence of the mechanism of the sensitivity of the doping to the surface of nanocrystals.

Modifying the n and p-type character of ambipolar materials such as HgTe is possible by the same approach. Figure 3C shows how the electrical conductance of HgTe CQD films is shifted n or p (with respect to an arbitrary potential) by the surface treatment with cadmium and sulfide ions, and it is noteworthy that the shift is on the order of the bulk bandgap. The ambient stability of doping of a solvated quantum dot is first determined by the Fermi level of the environment. In humid air, this is likely determined by the oxygen/water equilibrium, around +0.81 V/NHE (= +0.58 V vs Ag/AgCl = +0.17 V vs Fc/Fc^+) at neutral pH. Electrons below this potential are unstable to oxidation. As shown in Figure 2A, the HgS films are easily electron doped at this potential, and therefore air stability is indeed established. However, the absence of p-doping is limited by the oxidative decomposition of HgS.[19] Using the free energy of formation of HgS, ΔG^0_f, and the standard redox potential of Hg^{2+}, E^0, one can estimate the oxidation potential for $(HgS)_n + 2h^+ \rightarrow (HgS)_{n-1}S + Hg^{2+}$ (solvent) as +1 V/NHE from $E = \Delta G^0_f /2F + E^0$, where F is the Faraday constant (SI). Therefore at a potential just above where electrons are injected, hole injection would already lead to oxidative decomposition. This may explain why HgS CQDs are not ambipolar unlike HgTe CQDs. For dots in a film, in contrast to dots in solution, the spatial extent of the electrostatic potential can be much larger and the doping stability is determined by the diffusion of oxidizing or reducing species such that films could still be n or p- type even though the isolated dots may be unstable.

Returning to the possibility of using the intraband transitions, the consequence of the stable doping is that it transforms the "wide" gap β-HgS (0.6 eV as shown above) to a narrow gap semiconductor where the gap is now between the two first electronic states, $1S_e$ and $1P_e$ in spherical dots. This opens up the possibility of photophysical investigation of devices based on the permanent stable intraband absorption. One striking observation is the first detection of the intraband photoluminescence (PL) of HgS CQD. In Figure 3D, the PL emission overlaps the intraband absorption peak. The quantum yield is small, estimated at $\sim 10^{-3}$–10^{-4}, but it is similar to HgTe quantum dots with the same interband emission energy.[20] Intraband PL is easily seen in the β-HgS nanocrystals of varying sizes. The intensity depends strongly on the surface exposure (Figure S7) and it will be the subject of further studies. Interband PL has not been observed with either S^{2-} or Hg^{2+} exposure but only after the growth of a CdS shell. The lack of interband PL with sulfide exposure may be attributed to hole traps (filled electron states above the valence band states). This is the case for other semiconductors such as CdSe after sulfide treatment. With Hg^{2+} exposure, the $1S_e$ electrons should lead to 2electron−1hole Auger processes to also quench the interband PL.

It is noted that heavily doped nanocrystals that are not in the strong confinement regime exhibit infrared absorptions that are plasmons.[21] This applies to nonstochiometric copper chalcogens,[22] heavily doped Al:ZnO nanocrystals,[23] or phosphorus-doped silicon nanocrystals.[24] These plasmonic transitions exhibit no quantum confinement, no clear transfer of oscillator strength, no extensive size tuning, and no luminescence, unlike the intraband transitions and therefore cannot explain the observations on β-HgS nanocrystals studied here, which are strongly confined quantum dots and not in the heavily doped regime. It is also noted that the effects reported here cannot be assigned to some trap state unless such trap states would have many novel properties described above including optical absorption strength on par with interband transitions.

In summary, stable doping of colloidal quantum dots is an initial step toward the utilization of their intraband transitions, and this study on β-HgS showed the first colloidal quantum dots with stable electron occupation in the lowest quantum state in ambient conditions, and the appearance of intraband luminescence. The surface control of doping is demonstrated by optical, spectroelectrochemical and conductivity studies. This study shows a clear example where the large surface-to-volume ratio in nanomaterials is used advantageously to control the carrier doping. The strong modulation of the doping with alternating anions and cations via layer-by-layer growth is assigned primarily to energy level shifts of the quantum dot due to a surface dipolar layer.

■ ASSOCIATED CONTENT

Supporting Information

Experimental methods of synthesis, infrared absorption spectroscopy, difference spectroscopy, cyclic voltammetry, conductivity measurement, transmittance electron microscopy, X-ray diffraction spectroscopy, inductively coupled plasma optical emission spectrometry (ICP), photoluminescence measurement, and resting potential measurement. The size-dependent intraband-interband correlation, the figure of absorption spectra, mid-IR intraband photoluminescence with alternating Hg^{2+} and S^{2-} exposure, the table of ICP of Hg^{2+} and S^{2-} treated HgS CQDs, conductivity of HgTe CQD film and HgS CQD film with alternating surface exposure, $k \cdot p$ prediction in Figure 2B of the main manuscript, and electrochemical stability range of doped colloidal quantum dot. This material is available free of charge via the Internet at http://pubs.acs.org.

■ AUTHOR INFORMATION

Corresponding Author

*E-mail: pgs@uchicago.edu.

Notes

The authors declare no competing financial interest.

■ ACKNOWLEDGMENTS

This work was supported by the US National Science Foundation (NSF; grant DMR-1104755). The authors made use of shared facilities supported by the NSF MRSEC Program under DMR-0820054.

■ REFERENCES

(1) Talapin, D. V.; Lee, J.-S.; Maksym, V.; Shevchenko, E. V. Prospects of Colloidal Nanocrystals for Electronic and Optoelectronic Applications. *Chem. Rev.* **2010**, *110*, 389−458.
(2) Norris, D. J.; Efros, A. L.; Erwin, S. C. Doped Nanocrystals. *Science* **2008**, *319*, 1776−1779.
(3) Mocatta, D.; Cohen, G.; Schattner, J.; Millo, O.; Rabani, E.; Banin, U. Heavily Doped Semiconductor Nanocrystals Quantum Dots. *Science* **2011**, *332*, 77−81.
(4) Shim, M.; Guyot-Sionnest, P. N-type Colloidal Semiconductor Nanocrystals. *Nature* **2000**, *407*, 981−983.
(5) Keuleyan, S.; Lhuillier, E.; Guyot-Sionnest, P. Synthesis of Colloidal HgTe Quantum Dots for Narrow Mid-IR Emission and Detection. *J. Am. Chem. Soc.* **2011**, *133*, 16422−16424.
(6) Ithurria, S.; Talapin, D. V. Colloidal Atomic Layer Deposition (c-ALD) using Self-limiting Reactions at Nanocrystals Surface Coupled to Phase Transfer between Polar and Nonpolar Media. *J. Am. Chem. Soc.* **2012**, *134*, 18585−18590.
(7) Yu, D.; Wang, C.; Guyot-Sionnest, P. N-type Conducting CdSe Nanocrystal Solids. *Science* **2003**, *300*, 1277−1280.
(8) Shim, M.; Guyot-Sionnest, P. Intraband Hole Burning of Colloidal Quantum Dots. *Phys. Rev. B* **2001**, *64*, 245342.
(9) Liu, H.; Keuleyan, S.; Guyot-Sionnest, P. N- and p-type HgTe Quantum Dot Films. *J. Phys. Chem. C* **2012**, *116*, 1344−1349.
(10) Madelung, O. *Semiconductors Basic Data*; Springer-Verlag, Berlin, 2003.
(11) Eychmuller, A.; Hasselbarth, A.; Weller, H. Quantum-Size HgS in Contact with Quantum-Sized CdS Colloids. *J. Lumin.* **1992**, *53*, 113−115.
(12) Schooss, D.; Mews, A.; Eychmueller, A.; Weller, H. Quantum-Dot Quantum Well CdS/HgS/CdS: Theory and Experiment. *Phys. Rev. B* **1994**, *49*, 17072−17078.
(13) Higginson, K. A.; Kuno, M.; Bonevich, J.; Qadri, S. B.; Yousuf, M.; Mattoussi, H. Synthesis and Characterization of Colloidal β-HgS Quantum Dots. *J. Phys. Chem. B* **2002**, *106*, 9982−9985.
(14) Virot, F.; Hayn, R.; Richter, M.; Van den Brink, J. Engineering Topological Surface States: HgS, HgSe, and HgTe. *Phys. Rev. Lett.* **2013**, *111*, 146803.
(15) Kim, D. K.; Fafarman, A. T.; Diroll, B. T.; Chan, S. H.; Gordon, T. R.; Murray, C. B.; Kagan, C. R. Solution-Based Stoichiometric Control over Charge Transport in Nanocrystalline CdSe Devices. *ACS Nano* **2013**, *7*, 8760−8770.
(16) Yuan, M.; Zhitomirsky, D.; Adinolfi, V.; Voznyy, O.; Kemp, K. W.; Ning, Z.; Lan, X.; Xu, J.; Kim, J. Y.; Dong, H.; Sargent, E. H. Doping Control Via Moleculary Engineered Surface Ligand Coordination. *Adv. Mater.* **2013**, *25*, 5586.
(17) Kim, D. K.; Vemulkar, T. R.; Oh, S. J.; Koh, W. -K.; Murray, C. B.; Kagan, C. R. Ambipolar and Unipolar PbSe Nanowire Field-Effect Transistors. *ACS Nano* **2011**, *5*, 3230−3236.
(18) Campbell, I. H.; Rubin, S.; Zawodzinski, T. A.; Kress, J. D.; Martin, R. L.; Smith, D. L.; Barashkov, N. N.; Ferraris, J. P. Controlling Schottky Energy Barriers in Organic Electronic Devices Using Self-Assembled Monolayers. *Phys. Rev. B* **1996**, *54*, 14321−14324.
(19) Gerischer, H. On the Stability of Semiconductor Electrodes against Photodecomposition. *J. Electroanal. Chem.* **1977**, *82*, 133−143.
(20) Keuleyan, S.; Kohler, J.; Guyot-Sionnest, P. Photoluminescence of Mid-Infrared HgTe Colloidal Quantum Dots. *J. Phys. Chem. C* **2014**, *118*, 2749−2753.
(21) Scotognella, F.; Valle, G. D.; Kandada, A. R. S.; Zavelani-Rossi, M.; Comin, A.; Longhi, S.; Manna, L.; Lanzani, G.; Tassone, F. Plasmonics in Heavily-Doped Semiconductor Nanocrystals. *Eur. Phys. J. B* **2013**, *86*, 154.
(22) Zhao, Y.; Pan, H.; Lou, Y.; Qiu, X.; Zhu, J.; Burda, C. Plasmonic $Cu_{2-x}S$ Nanocrystals: Optical and Structural Properties of Copper-Deficient Copper (I) Sulfides. *J. Am. Chem. Soc.* **2009**, *131*, 4253−4261.
(23) Buonsanti, R.; Llordes, A.; Aloni, S.; Helms, B. A.; Miliron, D. J. Tunabe Infrared Absorption and Visible Transparency of Colloidal Aluminum-Doped Zinc Oxide Nanocrystals. *Nano Lett.* **2011**, *11*, 4706−4710.
(24) Rowe, D. J.; Jeong, J. S.; Mkhoyan, A.; Kortshagen, U. R. Phosphorus-Doped Silicon Nanocrystals Exhibiting Mid-Infrared Localized Surface Plasmon Resonance. *Nano Lett.* **2013**, *13*, 1317−1322.